

# AN IMPROVED-SENSITIVITY RESONANT ACCELEROMETER WITH FISHBONE-SHAPED RESONATORS OF HIGHER VIBRATION MODES

Hong Ding and Jin Xie

The State Key Laboratory of Fluid Power and Mechatronic Systems, Zhejiang University, Hangzhou 310027, People's Republic of China

## ABSTRACT

This paper reports an improved-sensitivity resonant accelerometer with fishbone-shaped resonators of higher vibration modes. Different from conventional resonant accelerometer integrating with low-order vibrating resonators, our prototype utilizes higher-mode fishbone-shaped resonators based on the principle that higher vibration modes have a higher frequency sensitivity. The proposed fishbone-shaped resonator can realize the mode selection and frequency-tuning function according to the configuration of sensing and driving electrodes. So this resonant accelerometer has sensitivity improvable and adjustable function compared to state of the art. Experimental results demonstrate the average differential sensitivities spanning from 12.44Hz/g to 61.00Hz/g (Mode 1: 12.44Hz/g; Mode 2: 36.94Hz/g; Mode 3: 61.00Hz/g) and the average resonant frequencies are 116.47KHz at mode 1, 299.87KHz at mode 2 and 548.35KHz at mode 3. Moreover, the tilt experiment verifies that this device has potential usage in tilt measurement.

## INTRODUCTION

MEMS resonators have a lot of applications, including timing [1], signal processing and wireless communication [2] etc. In these fields of applications, resonant accelerometer holds a unique position [3]. The resonator, as the core sensing element, alters its output resonant frequency as a function of the external acceleration because of the effect of inertial force on the equivalent stiffness. Resonant accelerometers possess various features, such as quasi-digital output signal, high sensitivity and large dynamic range, compared with the traditional capacitive accelerometer. In order to yield higher frequency sensitivity, previous research focused on the utilization and the optimization of micro-leverage mechanism [4]. For given conditions, the force amplification factor of an optimized micro-leverage is limited and invariable. That is the key restriction on the sensitivity improvement of the current state-of-the-art resonant accelerometers [3, 4].

Previous studies have found that for a resonant accelerometer, increasing the vibration mode increases the absolute frequency sensitivity of the resonator [5]. The conventional electrical design of the resonator, including actuation topology and the structure of the driving and sensing electrodes, only determines the first mode of vibration beam. For beam resonators, the usage of support beams placed at several flexural-mode node points has been reported [6, 7], but the resonant beam can only vibrate at a specific mode and is not tunable. To achieve mode selection and frequency-tuning function, a fishbone-shaped clamped-clamped beam resonator has been demonstrated [8]. The resonator can vibrate at different resonant modes by setting the configuration of the

electrodes. Consequently, the combination of resonant accelerometer and fishbone-shaped clamped-clamped resonator will achieve the sensitivity improvement.

In this paper, an improved-sensitivity resonant accelerometer with fishbone-shaped resonators of higher vibration modes is presented. The proposed accelerometer incorporates a pair of fishbone-shaped clamped-clamped beam as the resonant sensing elements, a pair of one-stage micro-leverage mechanisms and a proof mass. The device is fabricated in a silicon-on-insulator (SOI) wafer. Different configurations of sensing and driving electrodes corresponds to different vibration modes. The measurement results show the average differential sensitivities spanning from 12.44Hz/g to 61.00Hz/g (Mode 1: 12.44Hz/g; Mode 2: 36.94Hz/g; Mode 3: 61.00Hz/g) and the average resonant frequencies are 116.47KHz at mode 1, 299.87KHz at mode 2 and 548.35KHz at mode 3. Compared with the previously reported resonant accelerometer, this is the first time to realize a resonant accelerometer with tunable higher-order vibrating resonator. In addition, a tilt experiment in detection range of  $\pm 90^\circ$  came out to prove that this device has potential usage in tilt measurement.

## DESIGN AND ANALYSIS

The structure of the resonant accelerometer with fishbone-shaped resonators is shown in Figure 1. This accelerometer consists of a proof mass, a pair of single-stage micro-leverage mechanisms and a pair of fishbone-shaped resonators. With the action of external acceleration, the proof mass will move together with the leverages so the inertial force will be amplified. The amplified inertial force is applied to the resonators, and the tensile or compressive stress will shift their resonant frequency. Thus the acceleration can be detected by measuring this frequency shift. The symmetrical design and the differential structure can effectively eliminate disturbance and temperature influence.

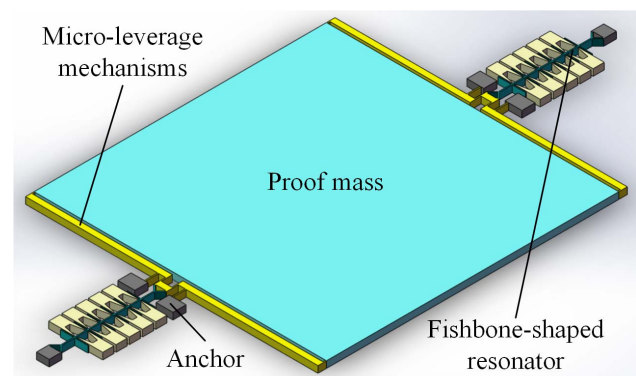


Figure 1: The scheme of resonant accelerometer with fishbone-shaped resonators.

The detailed drawing of the fishbone-shaped resonator is shown in Figure 2. The resonator consists of a main beam and six sub-beams along it. One end of the resonator is clamped to the anchor and the other one is connected to the output port of micro-leverage. Five pairs of tooth-shaped electrodes are placed facing to the sub-beams. If driving voltage is applied to certain combination of electrodes, different in-plane vibrational modes will come up.

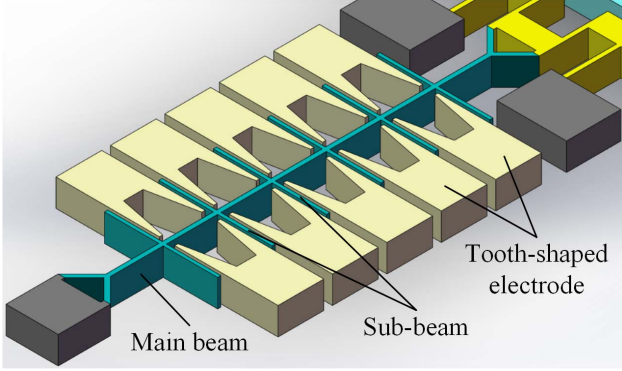


Figure 2: The scheme of fishbone-shaped resonator.

For the conventional parallel-plate or comb drive actuated beam resonators, the vibrating beams are driven by the distributed electrostatic force applied at the beam or the comb electrode. For the fishbone-shaped resonator, the electrostatic force is exerted on the sub-beams and causes its bending. On one hand, this bending generates a torque on the main beam, leading to its in-plane vibration. On the other, this vibration causes the shake of the sub-beams, the subsequent variation of the gap between the sub-beams and the electrode generates the motional current  $i(t)$  by which the vibration can be detected. Depending on both the number and the location of the electrodes, mode 1 to mode 3 can be excited.

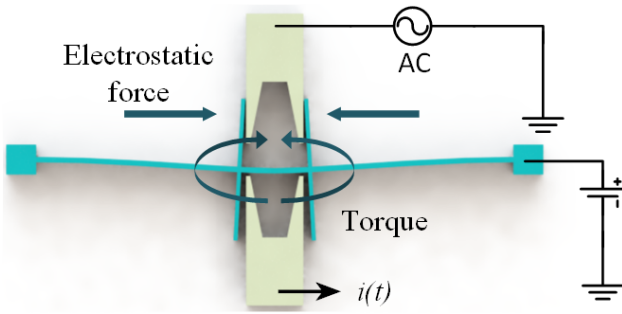


Figure 3: The working principle of the fishbone-shaped resonator.

The sensitivities of each vibration mode can be calculated from the frequency shift of the resonator at the axial loading. The variation of resonant frequency can be evaluated by a dynamic differential equation as [5]:

$$\left( \int_0^L \rho A \dot{\phi}_i^2 dx + \sum_j m_j \dot{\phi}_i^2(x_j) \right) \ddot{q}_i + \left( \int_0^L EI \left( \frac{\partial^2 \phi_i}{\partial x^2} \right)^2 dx + \int_0^L F \left( \frac{\partial \phi_i}{\partial x} \right)^2 dx \right) q_i = 0 \quad (1)$$

where  $\rho$ ,  $L$ ,  $A$ ,  $E$  and  $I$  are the density, the length, the sectional area, the Young's modulus and the moment of inertia of the main beam respectively,  $F$  is the axial tension force applied to the beam,  $m_j$  is the  $j$ th mass of sub-beam and  $x_j$  is its position,  $\phi_i$  is the  $i$ th mode shape, and  $q_i$  is the associated modal coordinate. The effective mass and the effective stiffness can be defined as [5]:

$$M_{eff} = \int_0^L \rho A \dot{\phi}_i^2 dx + \sum_j m_j \dot{\phi}_i^2(x_j) \quad (2)$$

$$K_{eff} = \int_0^L EI \left( \frac{\partial^2 \phi_i}{\partial x^2} \right)^2 dx + \int_0^L F \left( \frac{\partial \phi_i}{\partial x} \right)^2 dx$$

So the resonant frequency of the mode being analyzed under the axial force is:

$$f_n = \sqrt{\frac{K_{eff}}{M_{eff}}} \quad (3)$$

## FABRICATION

The SOI process has been chosen. The SOI wafer consists of a device layer, a buried oxide layer and a thick handle layer (Figure 4(a)). Through a lift-off process, the gold metal stack is patterned as conductive electrodes (Figure 4(b)). Via lithographic process followed with deep reactive ion etching (DRIE), the mechanical structures turns up in the device layer (Figure 4(c) and (d)). After this, the photo-resist is removed (Figure 4(e)). In order to releasing the moving parts of mechanical structures, the bare oxide layer is etched from the top surface by the process of vapor hydrogen fluoride (HF) (Figure 4(f)). Finally, as shown in Figure 5, the resonant accelerometer with fishbone-shaped resonators is fabricated.

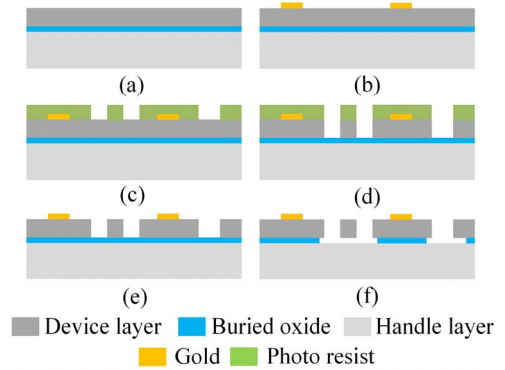


Figure 4: Fabrication process flow.

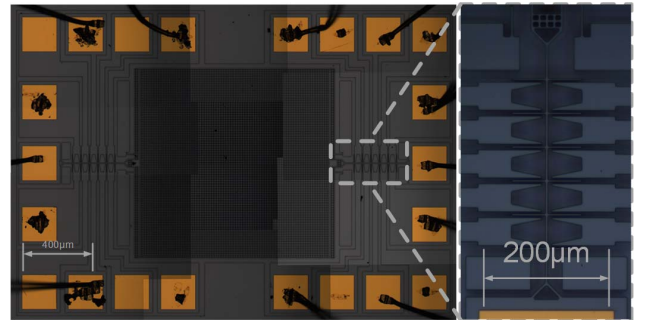


Figure 5: Overall and detailed optical microscope photo-graph of the device.

## EXPERIMENTS

The illustration of the resonator open-loop spectral response measurement setup is shown in Figure 6. The device is fixed on a remote-control rotation platform in a vacuum chamber with pressure level of 7.5mTorr at room temperature. The network analyzer swept frequency and tested the frequency response of the resonator. The gain of the transimpedance amplifier is  $10^6$  V/A. A DC polarization voltage  $V_p$  is applied on the anchor, and the AC actuation voltage  $v_{in}(t)$  is applied on the driving electrode. For different mode, the values of  $V_p$  and  $v_{in}(t)$  depend on the consideration of noise and nonlinearity.

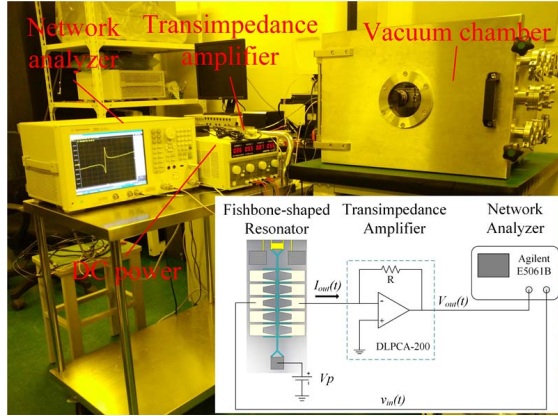


Figure 6: Measurement setup for resonator open-loop spectral response.

Figure 7 indicates the first to the third resonant mode so that the mode selection function is realized. The first mode electrode configuration needs one driving electrode and one sensing electrode. The configurations of the second and third modes are similar. The driving and the sensing electrodes are opposite and the electrode-pair is placed at the specific flexural-mode node point.

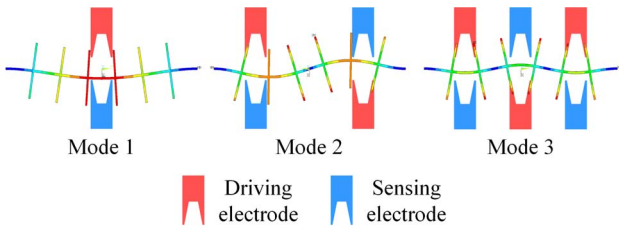


Figure 7: Mode selection principle and beam deformations at different modes.

By setting the configuration of the electrodes, the resonant modes 1 to 3 are achieved. The spectral response measurements are simply obtained with the rotation platform and repeated for 0 and  $\pm 1g$  in one axis. The results are reported in Figures 8 (a) - (f). These two fishbone-shaped resonators on the same axis incur opposite frequency shift for the induced accelerations consequently, validating the differential operation of the resonant accelerometer. The average sensitivities of modes 1 to 3 are 12.44Hz/g, 36.94Hz/g and 61.00Hz/g at average resonant frequencies of 116.47kHz, 299.87kHz and 548.35kHz respectively. It is clear that the sensitivity has risen as the vibration mode increases. In particular, the obtained performance are summarized as shown in Table

1. Owing to the use of fishbone-shaped resonator, the present device has higher sensitivity at higher mode and can adjust the sensitivity.

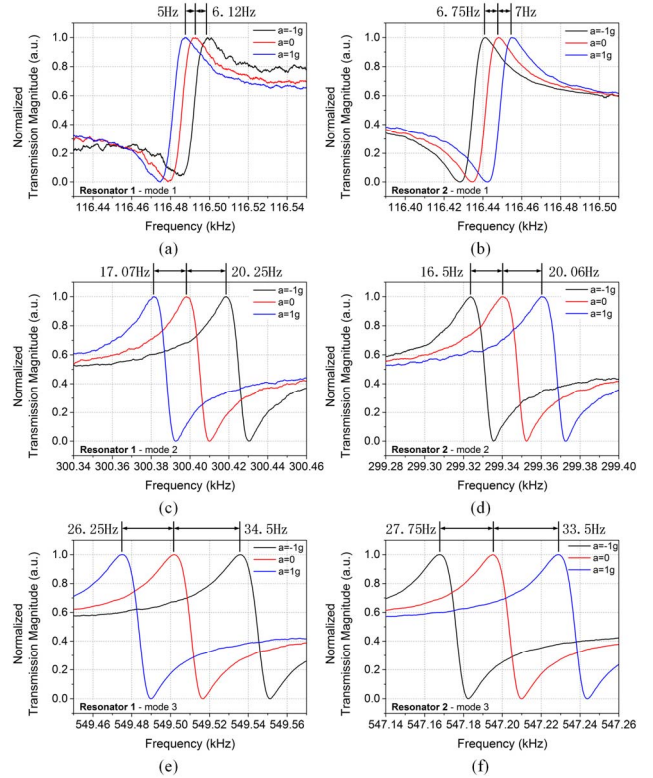


Figure 8: Normalized spectrum response of each single fishbone-shaped resonator evaluated for applied accelerations of  $\pm 1g$  at modes 1 to 3.

Table 1. Comparison of each resonant mode.

Mode	1	2	3
Resonant Frequency (kHz)	116.47	299.87	548.35
Sensitivity (Hz/g)	12.44	36.94	61.00

Figures 9 (a) and (b) show device response to multiple tilt angles for each resonator at modes 1 to 3. The two resonators on the same axis incur opposite frequency shift for the induced tilt angle consequently. The component force generated by the proof mass is given by:

$$F_{proof} = M_{proof} g \times \sin\theta \quad (4)$$

where  $M_{proof}$  is the proof mass,  $g$  is the gravitational acceleration and  $\theta$  is the tilt angle.

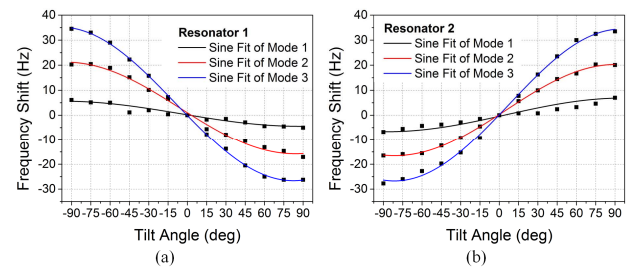


Figure 9: Multi-angle tilt test experimental results of each single fishbone-shaped resonator at modes 1 to 3.

It is clear that all the output responses match well with sine function of the tilt angle with a measurement range of  $\pm 90^\circ$ . The error mainly lies within the positioning accuracy of the rotation platform. Therefore, this device has potential usage in the tilt measurement with higher and adjustable sensitivity.

## CONCLUSIONS

An improved-sensitivity resonant accelerometer with fishbone-shaped resonators of higher vibration modes has been designed, fabricated and tested. The device is fabricated in an SOI wafer and experimented in vacuum chamber. The experimental results show the new resonant accelerometer has the average differential sensitivities from 12.44Hz/g to 61.00Hz/g (Mode 1: 12.44Hz/g; Mode 2: 36.94Hz/g; Mode 3: 61.00Hz/g) and the average resonant frequencies are 116.47KHz at mode 1, 299.87KHz at mode 2 and 548.35KHz at mode 3. Compared with the previous research, the present resonant accelerometer has higher and adjustable sensitivity due to the use of fishbone-shaped clamped-clamped beam resonator. In addition, this device can further be employed as a higher- and adjustable-sensitivity tilt sensor. Future work will focus on mode switch and frequency readout circuit to build a complete acceleration measurement system.

## ACKNOWLEDGEMENTS

This work is supported by the “National Natural Science Foundation of China (51475423)”, the “Zhejiang Provincial Natural Science Foundation of China (No.: LY14E050018)” and the “Science Fund for Creative Research Groups of National Natural Science Foundation of China (No.: 51521064)”.

## REFERENCES

- [1] C. T.-C. Nguyen, “MEMS technology for timing and frequency control”, in *The 2005 IEEE International Frequency Control Symposium and Exposition Conference*, Vancouver, August 29-31, 2005, pp. 251-270.
- [2] R. Liu, J. N. Nilchi, W. C. Li, C. T.-C. Nguyen, “Soft-impacting micromechanical resoswitch zero-quiescent power AM receiver”, in *MEMS 2016*, Shanghai, January 24-28, 2016, pp. 51-4.
- [3] H. Ding, J. Zhao, B. Ju, J. Xie, “A high-sensitivity biaxial resonant accelerometer with two-stage microleverage mechanisms”, *Journal of Micromechanics and Microengineering*, vol. 26, pp. 15-25, 2016.
- [4] S. X. Su, “Compliant leverage mechanism design for MEMS applications”, University of California, Berkeley, 2001.
- [5] T. Roessig, “Integrated MEMS tuning fork oscillators for sensor applications”, University of California, Berkeley, 1998.
- [6] M. U. Demirci, C. T.-C. Nguyen, “Higher-mode free-free beam micromechanical resonators”, in *IEEE International Frequency Control Symposium and PDA Exhibition Jointly with the 17th European Frequency and Time Forum*, Tampa, May 4-8, 2003,

pp. 810-818.

- [7] L. Shao, M. Palaniapan, W. Tan, L. Khine, “Nonlinearity in micromechanical free-free beam resonators: modeling and experimental verification”, *Journal of Micromechanics and Microengineering*, vol. 18, pp. 25-36, 2008.
- [8] N. Suzuki, H. Tanigawa and K. Suzuki, “Higher-order vibrational mode frequency tuning utilizing fishbone-shaped microelectromechanical systems resonator”, *Journal of Micromechanics and Microengineering*, vol. 23, pp. 45-55, 2013.

## CONTACT

\*Jin Xie, tel: +86-571-87952274; xiejin@zju.edu.cn